Yang, X., Chen, Q., Zhang, J.S, Magee, R., Zeng, J. and Shaw,C.Y. 2001. "Numerical simulation of VOC emissions from dry materials," *Building and Environment*, 36(10), 1099-1107.

Numerical simulation of VOC Emissions from Dry Materials

X. Yang[1*], Q. Chen[1], J.S. Zhang[2], R. Magee[2], J. Zeng[2], and C.Y. Shaw[2]

1 Building Technology Program, Massachusetts Institute of Technology, 77 Massachusetts Avenue, Cambridge, MA 02139, USA
2 National Research Council of Canada, Institute for Research in Construction, Indoor Environment Program, M-24, Montreal Road, Ottawa, Ontario K1A 0R6, Canada
* Current address: Department of Civil, Architectural, and Environmental Engineering, University of Miami, Coral Gables, FL 33124-0630, USA, Fax: (305) 284-3492

Abstract
This paper presents a numerical approach for simulating volatile organic compound (VOC) emissions from dry materials. The approach has been used to examine the VOC emissions from two particleboards. The emission study for the particleboards shows that a fairly good agreement of VOC concentrations between the model prediction and experimental data can be achieved by pre-calculating the partition coefficient (K_{ma}) and material age (AGE) and adjusting the diffusion coefficient (D_m) and initial concentration (C_0). Further, the study finds that K_{ma} only affects short-term emissions while D_m influences both the short-term and long-term emissions.

1. Introduction

Numerous field and laboratory studies have found that commonly used dry materials such as wood products, floor coverings (carpet, vinyl), wall coverings (wallpaper, fabric), ceiling materials (acoustic tiles, subfloors), and insulation materials (fiberglass, rigid foam) emit a variety of volatile organic compounds (VOCs). Emissions from dry materials are important to indoor air quality because of their large surface area and permanent exposure to indoor air. Therefore, they should be studied and rated so that only those with low emission rates are used in buildings.

In the past, VOC emissions from several hundred types of dry materials have been tested. These have been done mainly for screening purposes, *i.e.*, identifying the major VOCs emitted from a particular source and its time-varying emission dynamics. A majority of the tests use a small-scale test chamber under controlled environmental conditions (*e.g.*, 23 °C temperature, 50% relative humidity, and 1 air exchange per hour). A large body of measurement results can be found in the literature, and recently, have been included in the emission database of indoor materials [1, 2].

In addition to screening materials, the measurements should also:

(1) facilitate material ranking. Industries use the emission data to rank a material as a high, medium, or low emission source. This information can be given to material manufacturers for improving their products as well as to building designers to select the least toxic or non-toxic materials.

(2) help us understand emission characteristics. Contrary to "wet" materials, the emission rates of dry materials are usually small and decay slowly. This means that their emissions can last much longer than "wet" materials. The data would also help us to better understand emission mechanisms (*e.g.*, diffusion-controlled instead of evaporation- controlled).

(3) provide data for indoor air quality studies. Because limiting all the materials to zero- or low-emissions is either impractical or quite expensive, information on how to transfer the data from an environmental chamber to buildings is needed for indoor environment design.

The first two objectives can be easily achieved. The last one, however, cannot be inferred directly from the measured data due to the following two reasons:

(1) To obtain useful emission data for dry material, the test period must be sufficiently long. The real measurements cannot cover the entire emission life of a material. Material emissions beyond the period of measurement remain unknown.

(2) A chamber test usually measures a material sample. While in buildings, both the geometry (*e.g.*, the thickness of the material) and boundary conditions may be different from the test sample. Further, the environmental conditions in buildings may not be the same as those in a test chamber. Even though airflow may have a negligible effect, the diffusion process may be significantly affected by other factors, such as temperature. Hence, the measured data from an environmental chamber may not be valid in buildings.

Appropriate emission models are needed to solve the above problems. At present, most existing models for dry materials assume that emissions are exclusively dominated by internal diffusion. These existing models, so-called diffusion models, use Fick's law to solve VOC diffusions in a solid under simple initial and boundary conditions. For example, Dunn [3] calculates diffusion-controlled compound emissions from a semi-infinite source. Little *et al.* [4] simulates the VOC emissions from new carpets using the assumption that the VOCs originate predominately in a uniform slab of polymer backing material. These models, though based on the sound mass transfer mechanisms of VOC species, still have limitations:

(1) They presume that the only mass transfer mechanism is the diffusion through the source material. The models neglect the mass transfer resistance through the air phase boundary layer and also the air phase concentration on emissions. Although this may be true for some dry materials, the assumption as a general one has not been well justified.

(2) They tend to solve the VOC diffusion problem analytically. These models usually apply only to a 1-D diffusion process with simple boundary and initial conditions. In practice, emissions can be 3-D with complicated initial and boundary conditions.

Other than the above models, Yang *et al.* [5] developed a 2-D numerical model to simulate VOC emissions from an styrene-butadiene rubber (SBR) carpet. Their study considers the VOC mass transfer in both the material and the air phase boundary layer, but neglects the partition coefficient at the material-air interface. Use of the model is thus limited to materials with extremely small diffusivity or long-term emission evaluations.

The above indicates that, although there is general agreement that emissions from indoor sources can be described by fundamental mass transfer theories, a generalized model that has been validated with experimental data for detailed emission study is not yet available. This suggests a need for developing advanced models to fully characterize building material emissions and their impact on IAQ.

This paper presents a new strategy to developing a comprehensive mass transfer model without neglecting the mechanisms affecting dry material emissions. The model is a general one that applies to broad purposes, from obtaining useful material properties based on environmental chamber test data to studying material emissions in buildings.

2. The mathematical model

Consider a material source that has one surface exposed to the air. VOC emissions from the source include the mass transfer in three different regions [5]:

- The solid material
- The material-air interface
- The bulk air

2.1. Material layer

For a dry material with homogeneous diffusivity, several researchers [4 - 8] have used the following diffusion model to describe the VOC mass transport within the material:

$$\frac{\partial C_m}{\partial \tau} = \frac{\partial}{\partial x_j}\left(D_m \frac{\partial C_m}{\partial x_j}\right) \qquad (1)$$

where:
C_m = VOC concentration in the solid material, $\mu g/m^3$
τ = time, sec
x_j = coordinates (j = 1,2,3)
D_m = diffusion coefficient of the VOC in the solid material, m^2/s

Here, the dependence of D_m on the VOC concentration is usually neglected because the VOC concentrations in a dry source are usually very small (*e.g.*, the ratio of the initial VOC concentration to the material density is much less than the threshold 1%, as suggested by Schwope *et al.* [9]). The dependence of D_m on temperature can be assumed to follow an Arrhenius type [5]:

$$D_m = D_{m,0} \exp(-\frac{E_d}{RT}) \quad (2)$$

For a composite material composed of two or more layers of homogeneous materials, applying Eq. (1) to each layer yields:

$$\frac{\partial C_{m,i}}{\partial \tau} = \frac{\partial}{\partial x_j}(D_{m,i} \frac{\partial C_{m,i}}{\partial x_j}) \quad (3)$$

where i represents the i^{th} layer of the composite material. At the interface between the two layers, the VOC mass balance and the concentrations on the two sides take the form:

$$-D_{m,i} \frac{\partial C_{m,i}}{\partial x_j} = -D_{m,k} \frac{\partial C_{m,k}}{\partial x_j} \quad (4)$$

$$C_{m,i} = K_{ik} C_{m,k} \quad (5)$$

where i and k indicate two adjacent materials.

2.2. Material-air interface

At the material-air interface, a VOC phase change occurs from the material side to the air side. For low concentrations, the equilibrium condition at the material-air interface may be described by [8]:

$$C_m = K_{ma} C_a \quad (6)$$

where
K_{ma} = the dimensionless material-air partition coefficient.
C_a = the VOC concentration on the air side, mg/m^3

2.3. Air

The VOC mass transfer from the material-air interface to the ambient air is determined by velocity distributions as well as the flow type (*e.g.*, laminar or turbulent). For simplicity, the following discussion is confined to laminar flow (*e.g.*, flow in a small-scale chamber without a mixing fan).

For an incompressible, laminar, and Newtonian flow, the conservation equations for continuity, momentum (using Boussenisseq approximation for buoyancy), energy, and VOC species can be generalized as:

$$\frac{\partial}{\partial \tau}(\rho\phi) + \frac{\partial}{\partial x_j}(\rho u_j \phi) = \frac{\partial}{\partial x_j}(\Gamma_\phi \frac{\partial \phi}{\partial x_j}) + S_\phi \quad (7)$$

where

ρ = air density, kg/m^3
ϕ = 1 for mass continuity
ϕ = u_j (j = 1, 2, and 3) for three components of momentum (u,v,w)
ϕ = T for temperature
ϕ = C for VOC concentrations
x_j (j=1,2,3) = coordinate. In a cartecine coordinate, x_1=x, x_2=y, x_3=z
u_j (j=1,2,3) = three components of air velocity. In a Cartesian coordinate, u_1 = u (velocity in x direction), u_2 = v (velocity in y direction), u_3 = w (velocity in z direction)
Γ_ϕ = effective diffusion coefficient for ϕ
S_ϕ = source term for ϕ

The ϕ, Γ_ϕ and S_ϕ for different flows are shown in Table 1.

2.4. Boundary conditions

In addition to the above equations, appropriate boundary conditions are also needed. Although the boundary conditions for different problems vary, the four types of common boundary conditions of friction and VOC are inlet, outlet, walls, and axis of symmetry.

(a) Inlet

Air velocity (V) and compound concentration (C) are specified for the air supply inlet as:

$$V=V_{supply}$$
$$C=C_0 \quad (8)$$

where V_{supply} is air velocity at the supply inlet, and C_0 the inlet concentration (usually 0).

(b) Outlet

A pressure is given and zero gradient of compound concentration in the direction normal to the return outlet:

$$P=P_{return}$$
$$\frac{\partial C}{\partial x_j} = 0 \quad (9)$$

where P_{return} is the pressure at the return outlet and x_j is the coordinate normal to the outlet.

(c) Walls

Walls include solid walls of a test chamber (or room) and surfaces of the emission material. If V_i is air velocity parallel to a wall and x_j is the coordinate normal to the wall surface, the shear stress τ_w at a wall is expressed by:

$$\tau_w = -\mu \frac{\partial V_i}{\partial x_j} \tag{10}$$

The boundary condition for concentration at the emitting material surface is:

$$-D_m \frac{\partial C}{\partial x_j} = -D_a \frac{\partial C}{\partial x_j} \tag{11}$$

and at other non-emitting surfaces:

$$\frac{\partial C}{\partial x_j} = 0 \tag{12}$$

(d) Axis of symmetry

At the axis of symmetry, we have:

$$\frac{\partial C}{\partial x_j} = 0$$
$$\frac{\partial V_i}{\partial x_j} = 0 \tag{13}$$

where V_i is the air velocity perpendicular to the axis of symmetry, x_j.

The initial conditions for VOC are given as follows. In the air, the initial compound concentration is zero. In the solid material, we consider two different types of initial conditions:

$C = C_0$ for a new material: (14)

$C = C_0 F(x_j, AGE)$ for an aged material: (15)

where:

C_0 = initial concentration of compound in the solid slab, $\mu g/m^3$
AGE = age of the material, day
$F(x_j, AGE)$ = function used to describe the initial concentration profile in the solid

The key to using the above mathematical model for a dry material is to first obtain the physical properties of the material. These properties are a) the diffusion coefficient, D_m, b) the partition coefficient, K_{ma}, and c) the initial concentration, C_0. If the material is not totally new, the age of the material, AGE, is also needed. AGE specifies the initial condition of a dry material. AGE = 0 means a uniform initial concentration in the material while a non-zero AGE indicates a non-uniform initial concentration. Once these parameters are determined, they can be used to study the emissions under different environmental and boundary conditions (*e.g.*, in a building).

Before discussing the methods for obtaining the material properties, it is important to understand the influences of these key parameters on emissions from a dry source. The following section examines such influences.

3. The influence of C_0, D_m, K_{ma}, and AGE on dry material emissions

In this section, we present results using an example to study the sensitivity of dry material emissions to C_0, D_m, K_{ma}, and AGE.

A dry material with a dimension of $0.212 \times 0.212 \times 0.0159$ m^3 is placed in a small chamber of $0.5 \times 0.4 \times 0.25$ m^3, as shown in Figure 1. The chamber is ventilated by 1 ACH and the inlet concentration is 0. The only emitting area from the dry material is from the top surface (0.212×0.212 m^2), and the other faces of the material are well sealed. The physical properties of the material as a reference case are given as follows:

- $C_0 = 5.28\times10^7$ μg/m^3
- $D_m = 7.65\times10^{-11}$ m^2/s
- $K_{ma} = 3289$
- AGE = 0

The above parameters were obtained from those of a particleboard that is examined later. This section will examine the influence of each individual parameter (all the other parameters remain the same as those of the reference case) on the resulting VOC concentration at the chamber exhaust.

3.1. The influence of C_0

The mathematical model (Eqs. (1) - (15)) indicates that the VOC concentration in the chamber air depends linearly on the C_0. This can be confirmed by the results given in Figure 2. The figure shows that when C_0 increases from 5.28×10^7 μg/m^3 to 1.056×10^8 μg/m^3 (D_m, K_{ma}, and AGE remain the same as those in the reference case), the concentration also increases by a factor of 2.

3.2. The influence of D_m

Figure 3 illustrates the effect of D_m on the chamber concentration with time for a constant C_0 of 5.28×10^7 and K_{ma} of 3289 (AGE = 0). The values of D_m vary between 10^{-12} m^2/s and 10^{-10} m^2/s.

Results show that D_m significantly influences both the peak concentration and the decay rate of the concentration curve. A higher D_m results in a higher peak concentration and a faster decay rate.

3.3. The influence of K_{ma}

Figure 4 shows the effect of K_{ma} on the chamber concentration with time for a constant C_0 of 5.28×10^{7} and D_m of 7.65×10^{-11}(AGE = 0). The values of K_{ma} vary between 1 and 10,000.

Simulation results show that the influence of K_{ma} is two-fold. First, increasing the K_{ma} decreases the emission rate at early times and results in a slower depletion rate of the source. However, the influence of a change in K_{ma} is virtually insignificant below a value of about 1,000. On the other hand, it was observed that although the initial emission and depletion rates vary significantly for different K_{ma}, the chamber concentration after some time is almost identical. This suggests that for a dry source with small diffusivity, K_{ma} may only affect early-stage emissions.

To theoretically prove the above prediction, consider a dry material of thickness L that is exposed to air and emits VOCs. For simplicity, consider a 1-D problem only. The governing equation describing the transient diffusion through the material reads:

$$\frac{\partial C_m(y,\tau)}{\partial \tau} = D_m \frac{\partial^2 C_m(y,\tau)}{\partial y^2} \qquad 0<y<L,\ \tau>0 \qquad (16)$$

where
$C_m(y, \tau)$ = the VOC concentration at y and time τ
y = the coordinate in which direction that the VOC diffusion in the material takes place

At the material-air interface (y = L):

$$C_m(y=L,\tau) = K_{ma} C_a(y=L,\tau) \qquad (17)$$

$$q(y=L,\tau) = -D_m \frac{\partial C_m(y=L,\tau)}{\partial y} \qquad (18)$$

where $q(y, \tau)$ is the VOC emission rate (mg/m^2s) at the material-air interface and time τ.

At y = 0 we assume an adiabatic surface whereby:

$$\frac{\partial C_m(y=0,\tau)}{\partial y} = 0 \qquad (19)$$

The initial concentration in the solid material is given as uniform:

$$C_m(y,\tau=0) = C_{m0} = \text{const} \qquad 0<y<L \qquad (20)$$

Divide both sides of Eqs. (16) - (19) by C_{m0} and let:

$$\theta_m(y,\tau) = \frac{C_m(y,\tau)}{C_{m0}} \tag{21}$$

and

$$\theta_a(y = L,\tau) = \frac{C_a(y = L,\tau)}{C_{m0}} \tag{22}$$

Laplace transform Eqs. (16) - (19):

$$s\theta_m(y,s) - 1 = D_m \frac{d^2\theta_m(y,s)}{dy^2} \qquad 0<y<L,\ \tau>0 \tag{23}$$

$$\theta_m(y = L,s) = K_{ma}\theta_a(y = L,s) \tag{24}$$

$$Q(y = L,s) = -D_m \frac{d\theta_m(y = L,s)}{dy} \tag{25}$$

$$\frac{d\theta_m(y = 0,s)}{dy} = 0 \tag{26}$$

where s is time in the Laplace domain.

The solution to Eq. (23) that satisfies Eq. (26) is:

$$\theta_m(y,s) = \frac{1}{s} + A\cosh(y\sqrt{\frac{s}{D_m}}) \qquad 0<y<L \tag{27}$$

where A is a constant to be determined by boundary conditions

At y = L, we have from Eq. (27):

$$\theta_m(y = L,s) = \frac{1}{s} + A\cosh(L\sqrt{\frac{s}{D_m}}) \tag{28}$$

and

$$\frac{d\theta_m(y = L,s)}{dy} = A\sinh(L\sqrt{\frac{s}{D_m}}) \tag{29}$$

From Eqs. (25) and (29):

$$Q(y = L, s) = -A\sqrt{D_m s}\sinh(L\sqrt{\frac{s}{D_m}}) \tag{30}$$

From Eqs. (24) and (28), we can determine A as:

$$A = \frac{K_{ma}\theta_a(y = L, s) - \frac{1}{s}}{\cosh(L\sqrt{\frac{s}{D_m}})} \tag{31}$$

From Eqs. (30) and (31), we have the emission rate Q(y = L,s) in the Laplace domain:

$$Q(y = L, s) = -\sqrt{D_m s}\tanh(L\sqrt{\frac{s}{D_m}})[K_{ma}\theta_a(y = L, s) - \frac{1}{s}] \tag{32}$$

Eq. (32) indicates that the total emission in the Laplace domain, Q(y = L,s), is composed of two parts: due to the surface concentration, $K_{ma}\theta_a(y = L,s)$, and due to a step function, 1/s.

Initially (τ=0), $K_{ma}\theta_a(y = L, s) = \frac{1}{s}$ so Q(y = L,s) = 0.

As $\tau > 0$, the term $K_{ma}\theta_a(y = L,s)$ in Eq. (32) decreases as more VOCs are emitted out but the term 1/s remains constant. This means the contribution of the term $K_{ma}\theta_a(y = L,s)$ to emissions becomes less. At the point when

$$K_{ma}\theta_a(y = L, s) << \frac{1}{s} \quad ,$$

the effect of the surface concentration (hence K_{ma}) becomes negligible. The above proves that the K_{ma} does not affect the long-term emission of dry materials. Physically, the VOC concentration at the material surface approaches zero after sufficient time has elapsed.

3.4. The influence of AGE

The AGE is the time that it takes for a material with uniform initial concentration to reach the same initial VOC distribution as the material tested. In order to determine the impact of AGE on the subsequent emissions, a numerical simulation is conducted for a period of AGE by assuming the material is in the small-scale chamber. The concentration distributions in the material (which are not uniform) are then used as the initial condition for a new simulation. Results of the new simulation give the emissions by considering the material age.

Figure 5 gives the predicted VOC concentrations in the chamber outlet for different AGE. Results show that the emission rates for a smaller AGE are higher at the beginning. Meanwhile,

the figure also shows that the effect of AGE tends to diminish after a period. This indicates that the AGE affects only the early stage emissions.

4. Identification of material properties

The above sensitivity analysis indicates that in order to predict material emissions, all the material properties (C_0, D_m, K_{ma}, and AGE) must be properly obtained. In case these properties cannot all be accurately given, special attention should be paid to the C_0 and D_m because they determine both the short-term and long-term emission characteristics.

The most direct way of obtaining the material properties is by experimental measurements. Recently, Bodalol *et al.* [7] developed a method to measure the D_m and K_{ma} of dry sources. The method is promising in that it can provide a database of VOC transport properties for building materials. However, the measurements require a specially designed diffusiometer consisting of two stainless steel chambers (with the test specimen in between). Conducting the experiments is expensive and time consuming (it takes a long time for VOCs to diffuse through the specimen). Moreover, Bodalol [7] estimated that the measurement equipment has an uncertainty of ±18% for both D_m and K_{ma}. When the measured property values were used to predict emissions from the same material and VOCs, a much larger simulation error was observed [7].

Due to the limitations of the direct measurement approach, material properties can also be estimated by the use of emission chamber data (concentration vs. time curve) together with emission modeling through curve fitting. Since many chamber measurements have been conducted and published, obtaining material properties from the existing emission data is much cheaper than obtaining it from direct measurements. A major problem for this method is that it may involve obtaining two or more coupled unknowns using one set of data. However, results from the previous section indicate that the influence of C_0 on emissions can be separated from that of D_m, K_{ma}, and AGE. Among the last three, K_{ma} and AGE can be estimated in light of the following:

(a) Most materials tested are stored in a sealed tedlar bag from the time they are manufactured until they are tested. In such a case, AGE = 0.

(b) The short-term emissions of a dry material are not sensitive to the value of K_{ma} within a certain range (*e.g.*, 1 - 1,000) and the long-term emissions are independent of K_{ma}. This allows the use of some approximations to estimate K_{ma}, as demonstrated below.

If both AGE and K_{ma} can be pre-determined, the curve fitting will be for D_m only. In this way, the uncertainties of estimating two or more coupled parameters using one set of data can be eliminated.

In summary, the following procedures can be followed to obtain the material properties (D_m, K_{ma}, C_0) and material age (AGE) based on the measured emission data (C vs. τ) for a single sample of dry material.

Step 1: Analyze the emission data and identify the compound(s) emissions to be studied. Identify physical properties of the compound(s), such as molecular weight, vapor pressure, etc.

Step 2: Estimate AGE by tracking the material history and storage method.

Step 3: Pre-determine the material-air partition coefficient. Recently, Bodalal *et al.* [7] measured D_m and K_{ma} for several solid materials and found that although D_m depends heavily on both material and compound properties, the partition coefficient for different materials can be approximated based solely on the vapor pressure of the compound. Figure 6 shows the correlations for different materials and compounds given by Bodalal [7]. When the material and compound to be studied do not match the data available, the following correlation (for plywood) may be used:

$$K_{ma} = 10600 / P^{0.91} \tag{33}$$

where P is the vapor pressure of the compound in mmHg.

Step 4: Establish the computational domain, boundary and initial conditions.

Step 5: Use numerical simulation to obtain D_m by adjusting its value until the predicted chamber concentration agrees with the measured data. Since the initial concentration C_0 (which is unknown by now) does not affect the shape of the emission curve, at this stage we can assume an arbitrary value, $C_{0,ini}$ and compare the relative concentration (C/C_{max}) between the model prediction and the data. A least-square analysis is usually employed to obtain a "best fit" between the simulation results and the data. The D_m is obtained when a best fit is achieved.

Step 6: Obtain the initial concentration, C_0. Notice that the chamber concentration is proportional to C_0 for the same K_{ma} and D_m; the value of C_0 can be obtained by:

$$C_0 = C_{0,ini} \frac{C_{max,data}}{C_{max,sim}} \tag{34}$$

where $C_{max,data}$ and $C_{max,sim}$ are the maximum concentration by measurement and simulation, respectively.

In the following, the use of the above procedures are illustrated with two particleboard samples.

5. Application example: VOC emissions from particleboard

Particleboard is a panel product made of wood particles bounded together under heat and pressure, usually using an ureaformaldehyde (UF) resin adhesive. The adhesive produces a water-resistant bound. The bound is layered with the finer particles in the surface layers and coarser particles in the core layer.

Particleboards have long been identified as VOC emitters [10]. Recently, we measured the VOC emissions from two new particleboards. In the experiments, a small-scale chamber of $0.5\times0.4\times0.25$ m^3, illustrated in Figure 1, was used for measuring the particleboard emissions. Two different specimens of particleboard (PB1 and PB2) were tested. A sample holder was used in all the tests, limiting the exposure of the test specimens to a single face. Details of the test specimens and their geometrical dimensions are shown in Table 2. The test conditions were:

- Temperature: 23 ± 0.5 °C
- Relative humidity: 50 ± 0.5 %
- Air exchange rate: 1.0 ± 0.05 h^{-1}
- Loading ratio: 0.729 m^2/m^3

The tests lasted 96 hours for PB1, and 840 hours for PB2. The VOCs were screened by GC/MS and quantified by tube sampling and analyzed by GC/FID. Major compounds identified for the two different particleboards were the same: hexanal, α.pinene, camphene, and limonene.

For each particleboard tested, the emissions of TVOC and two major compounds: hexanal and α.pinene were simulated. Since both particleboards tested were new, the material age AGE = 0. K_{ma} was calculated using Eq. (33), and D_m and C_0 were obtained by curve fitting, as shown in Table 3.

Figures 7 and 8 compare the predicted VOC concentrations and the data using the properties listed in Table 3. An examination of the material property data revealed several interesting features:

(1) The VOC emission profiles between the two particleboards are very different. However, the property data in Table 3 indicate that the two particleboards actually shared the same partition coefficient (K_{ma}) and diffusion coefficient (D_m). The only difference is the initial concentration, C_0. The high initial concentration of the PB2 seems to be connected to the high percentage of scavenger (see Table 2) used during the manufacturing process. This suggests that an effective way to reduce emissions from the material is to use as little scavenger as possible to reduce C_0.

(2) For the two types of particleboards studied, K_{ma} and D_m for TVOC can be represented by those of hexanal, the most abundant compound in the particleboards.

(3) For both the two particleboards examined, emissions of α.pinene decayed faster than TVOC and hexanal. Hence, the D_m for α.pinene is larger than that of hexanal (1.2×10^{-10} vs. 7.65×10^{-11}). This finding however is contrary to the molecular diffusion theory. Based on the diffusion theory, compounds with larger molecular weight (α.pinene) should have a smaller diffusion coefficient. The reason for this unusual phenomenon is not clear.

6. Conclusions

This paper presents a numerical approach for simulating VOC emissions from dry materials. The approach uses the following parameters to describe emission characteristics: the initial VOC

concentrations in the material (C_0), the solid-phase diffusion coefficient (D_m), the material-air partition coefficient (K_{ma}), and the age of the material (AGE). The parameters were obtained by fitting the predicted VOC concentrations with the small-scale chamber data.

Our study finds that different parameters have different impacts on emissions. The emission rate is in proportion to C_0. D_m influences both short-term and long-term emissions. A higher D_m results in a higher initial emission rate and a faster decay rate. On the other hand, K_{ma} and AGE affect only the short-term emissions of the particleboard. It has virtually no impact to long-term emissions.

The emission studies for two different particleboard samples show that a fairly good agreement of VOC concentrations between the experimental data and model prediction can be achieved by pre-determining K_{ma} and AGE and adjusting D_m and C_0. These material properties obtained can be used to study material emissions in buildings, and help to reduce the material emissions by reformulating the products.

Acknowledgements

This investigation is supported by the US National Science Foundation (Grant CMS-9623864) and National Research Council of Canada.

References

[1] European Commission (EC), *European Data Base on Indoor Air Pollution Sources in Buildings*, Final Report, 1997.

[2] National Research Council (NRC), *MEDB-IAQ: Material Emission Database and a single-zone IAQ model – a tool for building designers, engineers, and managers*, IRC/NRC CMEIAQ Final Report 4.2, Ottawa, Canada, 1999.

[3] Dunn, J.E., Models and statistical methods for gaseous emission testing of finite sources in well-mixed chambers, *Atmospheric Environment*, 1987, **21**(2), 425-430.

[4] Little, J.C., Hodgson, A.T., and Gadgil, A.J., Modeling emissions of volatile organic compounds from new carpets, *Atmospheric Environment*, 1994, **28**(2), 227-234.

[5] Yang, X., Chen, Q. and Bluyssen, P.M., Prediction of short-term and long-term volatile organic compound emissions from SBR bitumen-backed carpet under different temperatures, *ASHRAE Transactions*, 1998, **104**(2), 1297-1308.

[6] Christianson, J., Yu, J.W. and Neretnieks, I., Emission of VOC's from PVC-flooring - models for predicting the time dependent emission rates and resulting concentrations in the indoor air, *Proceedings of Indoor Air'93*, 1993, **2**, 389-394.

[7] Bodalal, A., Fundamental mass transfer modeling of emission of volatile organic compounds from building materials, Ph.D. Thesis, Department of Mechanical and Aerospace Engineering, Carleton University, Canada, 1999.

[8] Yang, X., Study of building material emissions and indoor air quality, Ph.D. Thesis, Department of Architecture, Massachusetts Institute of Technology, Cambridge, MA, 1999.

[9] Schwope, A.D., Lyman, W.J., and Reid, R.C., Methods for assessing exposure to chemical substances, *Vol. 11: Methodology for estimating the migration of additives and impurities from polymetric materials*, U.S. Environmental Protection Agency, Office of Toxic Substances, Washington, DC, EPA/560/5-85-015, 1989.

[10] Matthews, T.G., Reed, T.J., Timberg, B.J., Daffron, C.R. and Hawthorne, A.R., Formaldehyde emissions from combustion sources and solid formaldehyde resin containing products: Potential impact on indoor formaldehyde concentrations and possible corrective measures, *Proceedings of An Engineering Foundation Conference on Management of Atmospheres in Tightly Enclosed Spaces*, Santa Barbara, ASHRAE, 1983, 23-43.

Table 1 Values of ϕ, Γ_ϕ and S_ϕ in Eq. (7).

ϕ	Γ_ϕ	S_ϕ
1	0	0
U_i (i=1,2,3)	μ	$-\frac{\partial p}{\partial x_i} - \rho g_i \beta (T - T_0)$
T	μ/Pr	S_T
C	μ/Sc	S_c
Where μ is laminar viscosity, Pa.s p is air pressure, Pa g_i is component i of the gravitation vector, m/s^2 β is thermal expansion factor, 1/K T_0 is reference temperature Pr= 0.71 is the Prandtl number Sc is the molecular Schmidt number		

Table 2 Test specimens of the particleboard.

Specimen	**Type/Grade**	**Length/width/height (m)**	**Manufacturing details**
PB1	Industrial	0.212×0.212×0.0159	Single opening line; 100s press UF Resin: 11.5% face, 8.9% core Scavenger: 15.0% face, 5.0 % core
PB2	Industrial	0.212×0.212×0.0159	Multi-opening line; 125s press UF Resin: 11.2% face, 9.4% core Scavenger: 35% face, 20 % core Wax: 1.2% face, 0.9% core

Table 3 Physical properties of particleboard emissions

(a) PB1

Compound	**TVOC**	**Hexanal**	**α.Pinene**
D_m (m^2/s)	7.65×10^{-11}	7.65×10^{-11}	1.2×10^{-10}
C_0 ($\mu g/m^3$)	5.28×10^{7}	1.15×10^{7}	9.86×10^{6}
K_{ma}	3289	3289	5602
AGE	0	0	0

(b) PB2

Compound	**TVOC**	**Hexanal**	**α.Pinene**
D (m^2/s)	7.65×10^{-11}	7.65×10^{-11}	1.2×10^{-10}
C_0 ($\mu g/m^3$)	9.86×10^{7}	2.96×10^{7}	7.89×10^{6}
K_{ma}	3289	3289	5602
AGE	0	0	0

Figure caption

Figure 1 A small-scale chamber for measuring dry material emissions.

Figure 2 The influence of the initial concentration of the source on the resulting VOC concentration in the chamber air. The curve is predicted with the diffusion coefficient D_m = 7.65×10^{-11} m^2/s, partition coefficient K_{ma} = 3289, and material age AGE = 0.

Figure 3 The influence of diffusion coefficient on the resulting VOC concentration in the chamber air. The curve is predicted with the initial concentration C_0 = 5.28×10^{7} $\mu g/m^3$, partition coefficient K_{ma} = 3289, and material age AGE = 0.

Figure 4 The influence of the material-air partition coefficient on the resulting VOC concentration in the chamber air. The curve is predicted with the diffusion coefficient D_m = 7.65×10^{-11} m^2/s, initial concentration C_0 = 5.28×10^{7} $\mu g/m^3$, and material age AGE = 0.

Figure 5 Comparison of VOC concentrations at the chamber outlet with different material age, AGE. The curve is predicted with the diffusion coefficient D_m = 7.65×10^{-11} m^2/s, partition coefficient K_{ma} = 3289, and initial concentration C_0 = 5.28×10^{7} $\mu g/m^3$.

Figure 6 Measured partition coefficient of different materials (Bodalal, 1999).

Figure 7 Comparison of measured and simulated VOC concentrations emitted from PB1: (a) TVOC, (b) Hexanal, (c) α.pinene.

Figure 8 Comparison of measured and simulated VOC concentrations emitted from PB2: (a) TVOC, (b) Hexanal, (c) α.pinene.

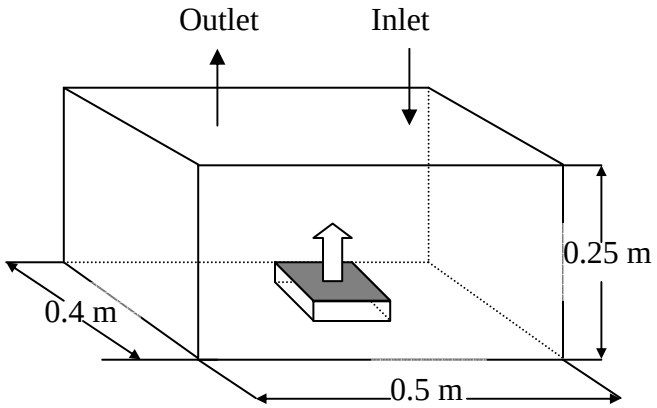

Figure 1 A small-scale chamber for measuring dry material emissions.

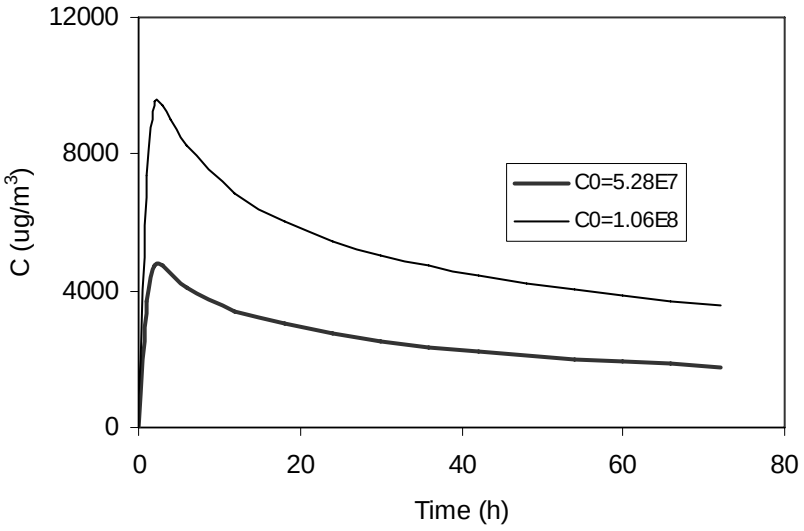

Figure 2 The influence of the initial concentration of the source on the resulting VOC concentration in the chamber air. The curve is predicted with the diffusion coefficient D_m = 7.65×10^{-11} m^2/s, partition coefficient K_{ma} = 3289, and material age AGE = 0.

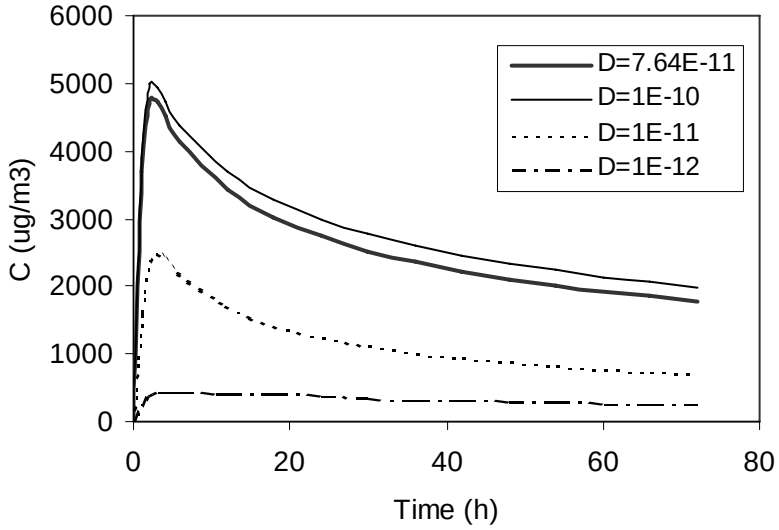

Figure 3 The influence of diffusion coefficient on the resulting VOC concentration in the chamber air. The curve is predicted with the initial concentration $C_0 = 5.28\times10^7$ μg/m^3, partition coefficient $K_{ma} = 3289$, and material age AGE = 0.

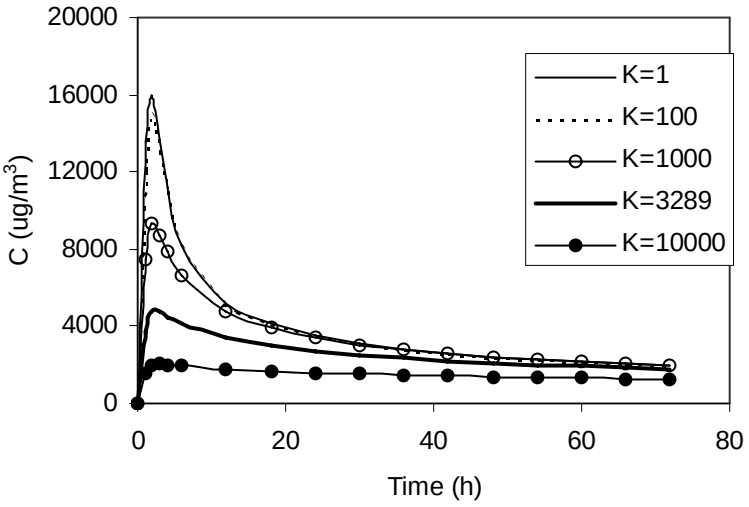

Figure 4 The influence of the material-air partition coefficient on the resulting VOC concentration in the chamber air. The curve is predicted with the diffusion coefficient D_m = 7.65×10^{-11} m^2/s, initial concentration $C_0 = 5.28\times10^7$ $\mu g/m^3$, and material age AGE = 0.

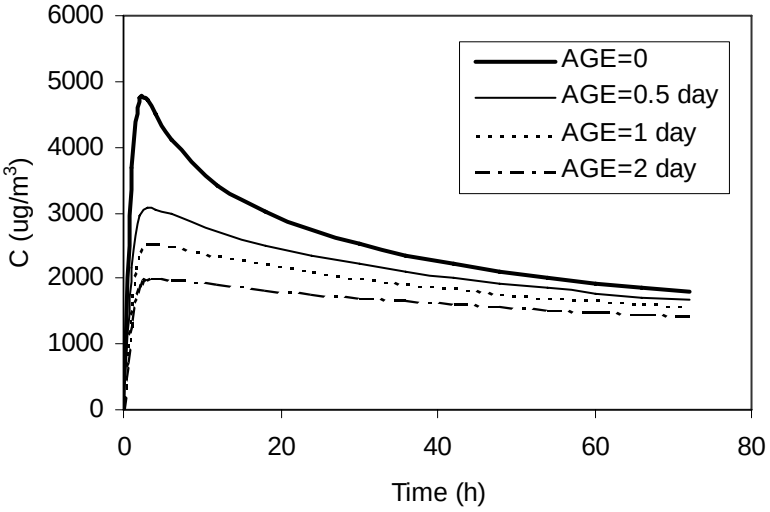

Figure 5 Comparison of VOC concentrations at the chamber outlet with different material age, AGE. The curve is predicted with the diffusion coefficient $D_m = 7.65\times10^{-11}$ m^2/s, partition coefficient $K_{ma} = 3289$, and initial concentration $C_0 = 5.28\times10^7$ $\mu g/m^3$.

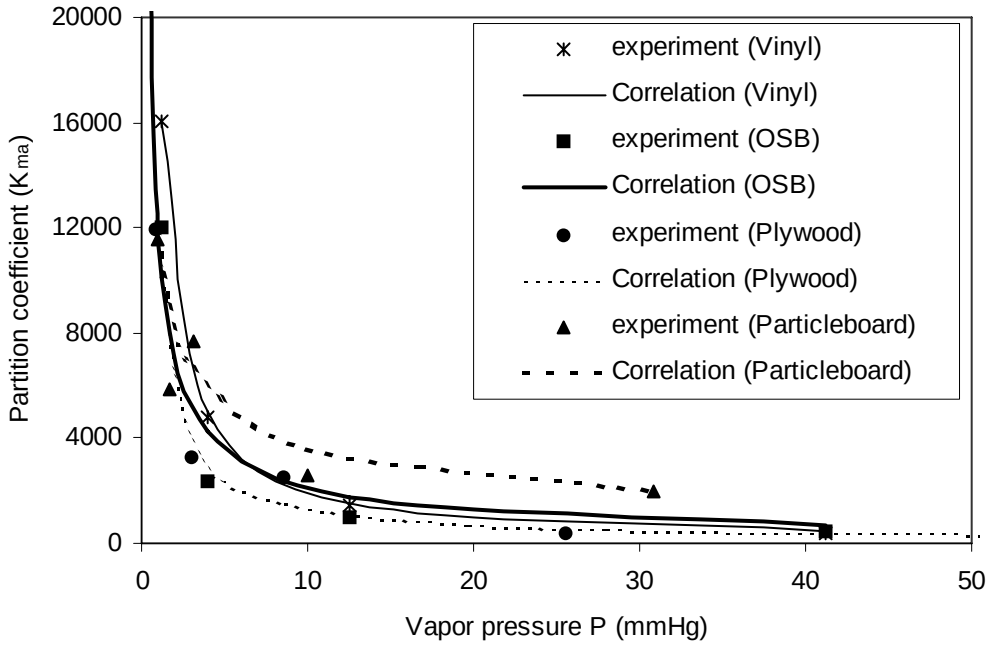

Figure 6 Measured partition coefficient of different materials (Bodalal, 1999).

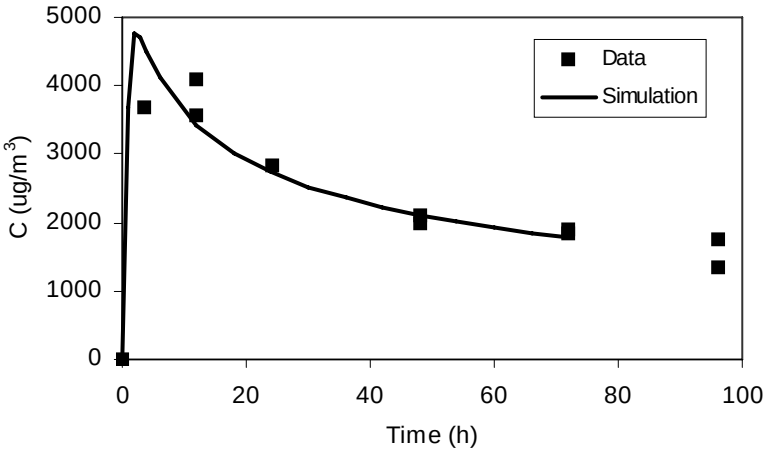

(a)

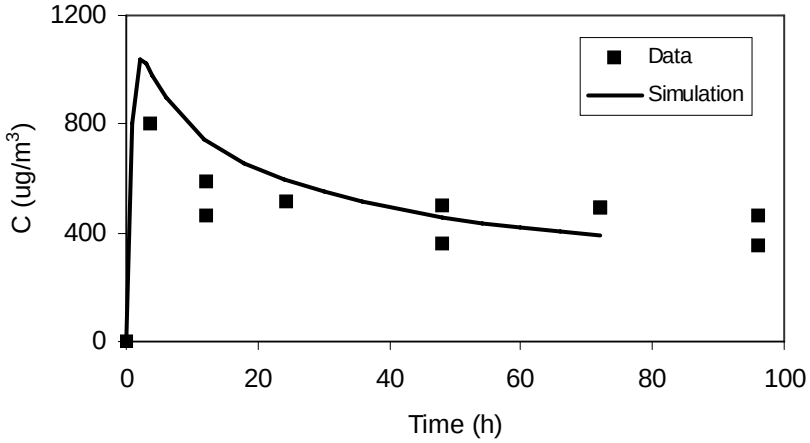

(b)

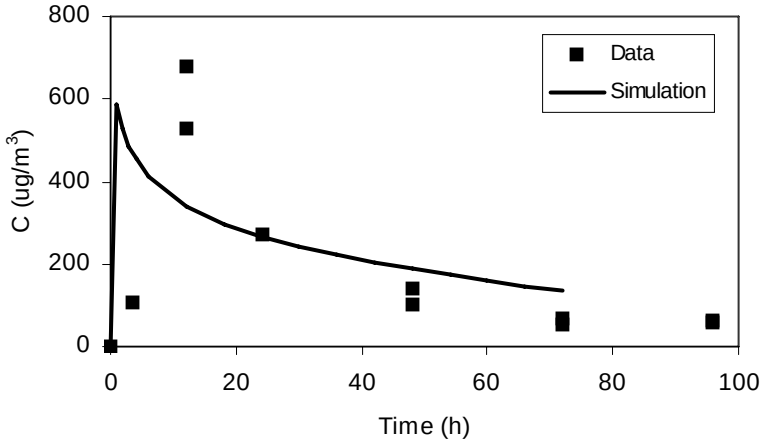

(c)

Figure 7 Comparison of measured and simulated VOC concentrations emitted from PB1: (a) TVOC, (b) Hexanal, (c) α.pinene.

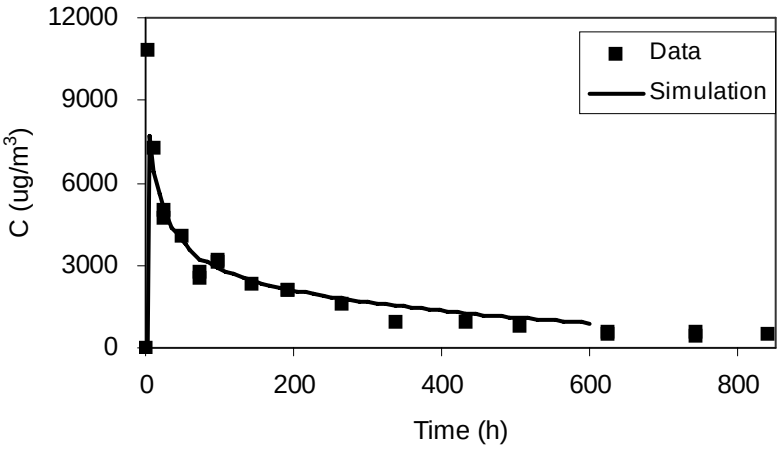

(a)

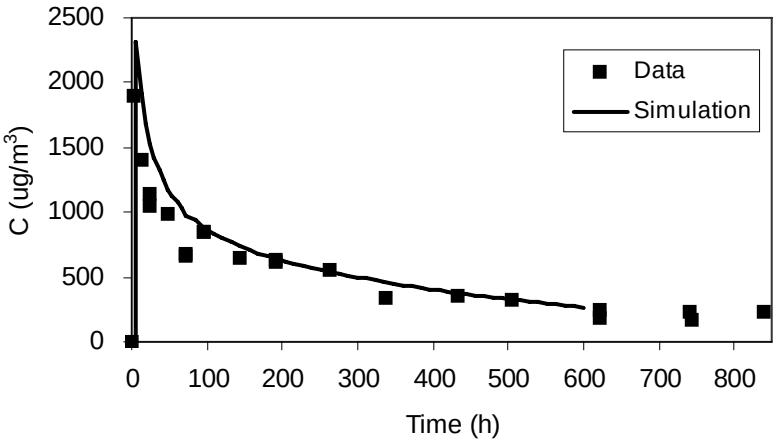

(b)

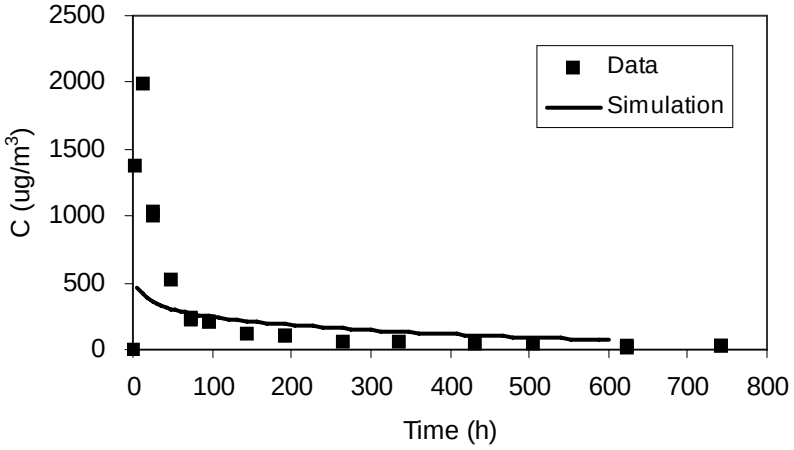

(c)

Figure 8 Comparison of measured and simulated VOC concentrations emitted from PB2: (a) TVOC, (b) Hexanal, (c) α.pinene.